

# Engineering Oriented Gases: The Mechanism of Dyeing Potassium Sulfate

Loyd D. Bastin and Bart Kahr\*

Department of Chemistry, University of Washington, Box 351700, Seattle, WA 98195-1700, USA

Received 17 November 1999; accepted 21 April 2000

**Abstract**—Potassium sulfate was crystallized from solutions containing mM quantities of a variety of sulfonated dye molecules that became encapsulated within particular growth sectors. Linear dichroism measurements of the crystals coupled with a knowledge of the absorption anisotropy of the dyes obtained from semi-empirical molecular orbital theory, enabled the determination of the orientation of at least one dye molecule within each of the principal growth sectors ( $\{010\}$ ,  $\{021\}$ ,  $\{110\}$ ,  $\{001\}$ ,  $\{111\}$ ) of  $K_2SO_4$ . The ensemble of orientations suggested a general mechanism of mixed crystal formation in which the dye's sulfonate groups matched the separation between sulfate ions in the lattice. The corresponding experiments with  $K_2SO_4$  isomorphs as well as the habit modification accompanying dye inclusion crystal (DIC) formation are discussed. We further demonstrate how sector specific recognition enables growing crystals to separate molecules from complex solutions. © 2000 Elsevier Science Ltd. All rights reserved.

## Introduction

Recently, great effort has been directed toward the design of molecular crystalline materials, especially by exploiting hydrogen bonds,<sup>1</sup> but the design of dilute solid solutions has received little attention even though for some optical applications molecules that are oriented and isolated from one another are requisite.<sup>2</sup> We have been seeking to identify the prevailing intermolecular forces that determine the formation of dye inclusion crystals (DICs), simple host crystals containing chromophores oriented and isolated in particular growth sectors. In this paper, we focus on placing sulfonated dyes within otherwise single  $K_2SO_4$  crystals in predetermined orientations.

Previously, we demonstrated by polarization spectroscopy that two trisulfonated dyes were oriented in  $K_2SO_4$  crystals in a manner that was consistent with a mixed crystal growth mechanism involving the stereoregular substitution of dye  $-SO_3^-$  groups for crystal  $SO_4^{2-}$  ions.<sup>3</sup> Because such a proposition is an oversimplification of complex interactions between large molecules and growing salt surfaces we were interested in determining whether we had struck on a reliable directing mechanism with predictive power that could be applied to dyes with more or fewer than three sulfonate substituents. We now have more than 100 sulfonated dyes within  $K_2SO_4$  crystals—some included through each of the principal growth surfaces ( $\{010\}$ ,  $\{021\}$ ,  $\{110\}$ ,  $\{001\}$ ,  $\{111\}$ )<sup>4</sup>—and are therefore in a position to address the generality and utility of the stereoregular  $-SO_3^- - SO_4^{2-}$

substitution mechanism in mixed crystal formation. Do the electrostatic forces that presumably drive the substitution stand out among other interactions and can they be invoked as a general engineering principle for dilute solid solutions as hydrogen bonds are used for molecular crystal engineering?

## Historical

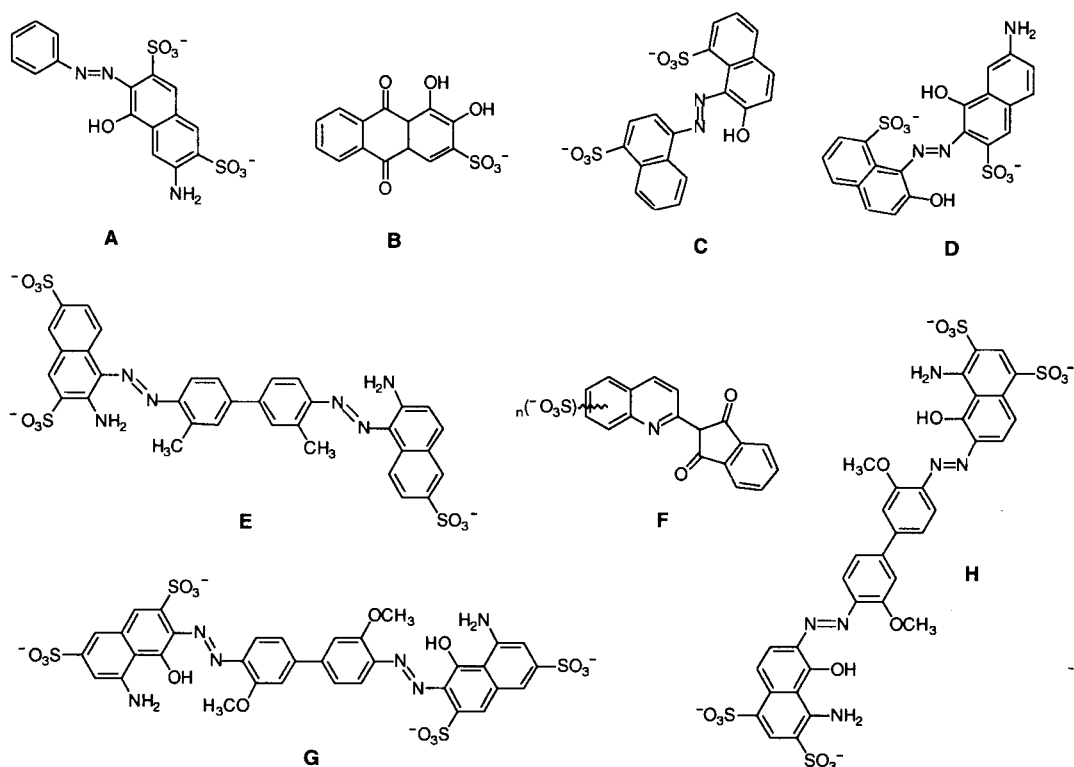
Natural dyes were first used to color salt crystals in an attempt to mimic pleochroism in minerals;<sup>5</sup> coal-tar dyes were subsequently introduced for this purpose.<sup>6</sup> Retgers first stained  $K_2SO_4$  crystals with bismarck brown, the only one of 26 dyes that did so.<sup>7,8</sup> Wenk studied bismarck brown and ponceau red among other dyes<sup>9</sup> in  $K_2SO_4$ , while Gaubert used ponceau red and safranin.<sup>10</sup>

Buckley first used sulfonated dyes or acid dyes for coloring  $K_2SO_4$  crystals<sup>11</sup> in the context of his pioneering studies of crystal habit modification. Following a series of papers on the influence of inorganic impurities on the habits of simple salt crystals, Buckley shifted his focus by using dyes as the habit modifying agents.<sup>12,13</sup> From more than 16,000 crystallizations, Buckley ranked dyes<sup>14</sup> in terms of their power to inhibit the growth rates of particular surfaces of crystals such as  $KClO_3$ ,  $K_2SO_4$ ,  $K_2CrO_4$ ,  $NH_4ClO_4$ , and  $KAl(SO_4)_2 \cdot 12H_2O$ .<sup>15</sup>

Having first observed that simple tetrahedral oxy-anions modified the habits of other oxy-anion containing crystals, Buckley surmised that the substitution of one  $XO_4^{n-}$  ion for another resulted in the slower growth of the faces where

Keywords: potassium sulfate; dyeing; mixed crystal growth.

\* Corresponding author. E-mail: kahr@chem.washington.edu



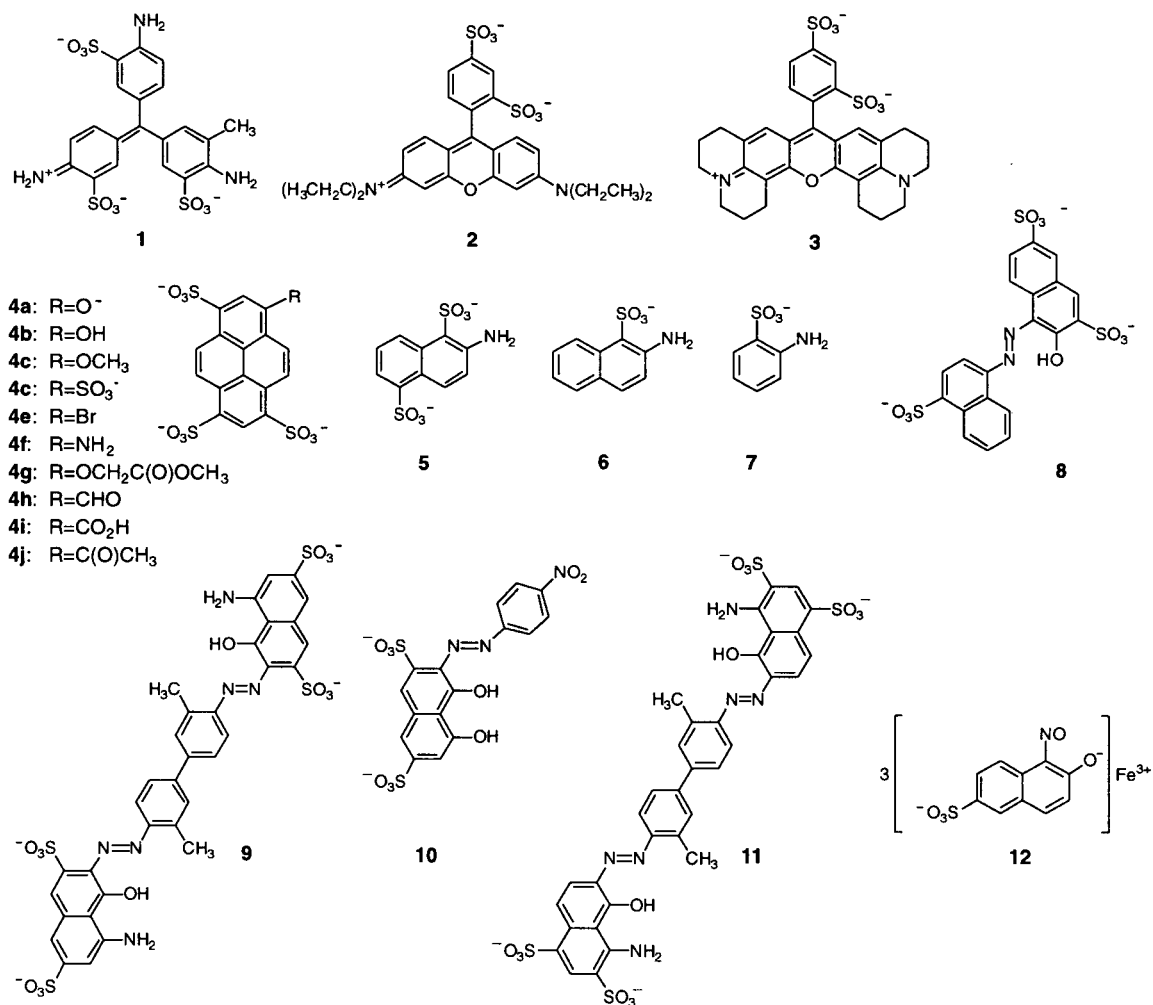
substitution was preferable. These judgments were complicated because some pairs of similarly shaped ions not only influenced the habits of the other's crystals but also formed mixed crystals. His switch to water soluble sulfonated dyes as habit modifying agents was predicated on the fact that given the gross dissimilarity in size and shape between the crystal ions and impurity ions, mixed crystal formation would undoubtedly be excluded by the Principle of Isomorphism<sup>16</sup> even though the requisite tetrahedral anionic functionality was present. Nevertheless, Buckley did observe the formation of salt crystals containing oriented dye molecules, a process that he viewed as both an annoyance and an opportunity. Such objects confounded his interpretation of habit modification, yet provided, in principle, a way to determine the orientation of the dye molecules with respect to the surfaces through which they adhered.

Buckley compiled tables of qualitative linear dichroism observations associated with dyes in the {010} growth sectors of  $K_2SO_4$ , among other crystals.<sup>17</sup> Examples of  $K_2SO_4$  DICs are illustrated in Buckley's book *Crystal Growth* and include the following: acid fuchsin (**1**, Colour Index number<sup>8</sup> (C.I. #) 42685), azo-orseille R (**A**, C.I. # 17160) and alizarin red (**B**, C.I. # 58005) in the {110} growth sectors, croceine scarlet 3BX (**C**, C.I. # 16050) and ponceau 3R (**D**, C.I. # 17110) in {021}, naphthol green (**12**, C.I. # 10020) in {001}, brilliant congo R (**E**, C.I. # 23570) in {111},<sup>18</sup> as well as quinoline yellow (**F**, C.I. # 47005) in indeterminate sectors.<sup>11</sup> In his final review,<sup>14</sup> Buckley presented the first photometric data from DICs, the optical absorption spectra for chromotrope 2B (**10**, C.I. # 16575) in  $K_2SO_4$ , collected with the electric vector of the polarized light parallel to each of the principal

directions. He acknowledged that these polarized absorption spectra would be useful in establishing a recognition mechanism but the data was never interpreted or elaborated upon. In the 1930s the conformational analysis and electronic structure of dyes were poorly understood; optical spectroscopies were exotic rather than routine. Nevertheless, by extension of his work with oxy-anion impurities, Buckley believed that the sulfonate groups were active in both habit modification and mixed crystal growth.

France, while studying the influence of dyes on alum crystals, adopted Buckley's  $-SO_3^- - SO_4^{2-}$  substitution mechanism.<sup>19</sup> With Rigtterink he described 11 specially prepared and purified isomeric azo dyes in  $K_2SO_4$  some of which produced well-defined, so-called hourglasses or bow ties of color by adsorption and overgrowth on the {110} planes.<sup>20</sup> Like Buckley, they were not able to offer definite structural or mechanistic conclusions. France was the first to carry out X-ray measurements on DICs but he could not detect differences between the pure salts and those containing dyes in 1 part in 1000.<sup>21</sup> Recently, Dudley and Vetter determined by synchrotron white beam X-ray topography that some dyed  $K_2SO_4$  crystals are remarkably indistinguishable from pure  $K_2SO_4$  grown under similar conditions, while others are highly mosaic.<sup>22</sup>

Whetstone, motivated to control the habits of  $NH_4NO_3$  crystals for use in explosives, studied the habit modifying effects of 120 dyes. Acid fuchsin (**1**) and its congeners were especially effective.<sup>23</sup> He developed structural models for various sulfonated dyes included within  $NH_4NO_3$  crystals predicated on stereoregular substitutions of dye sulfonates for crystal nitrates, a generalization of the  $-SO_3^- - SO_4^{2-}$  substitution mechanism of Buckley and France.<sup>24,25</sup> We

**Table 1.** Crystal growth conditions, composition, absorption maxima, and solution absorptivities

Dye	Dye:salt molar ratio in growth solutions	$\lambda_{\max}$ (nm)		$\epsilon$ (L M <sup>-1</sup> cm <sup>-1</sup> ) <sup>e</sup>	Salt:dye molar ratio
		Satd K <sub>2</sub> SO <sub>4</sub> soln	K <sub>2</sub> SO <sub>4</sub> crystal		
<b>1</b>	1.5×10 <sup>-4</sup>	508; 548	508; 563	2.2×10 <sup>4</sup>	5.4×10 <sup>4</sup>
<b>2</b>	2.9×10 <sup>-2</sup> <sup>a</sup>	533; 568	537 <sup>f</sup> ; 571	1.3×10 <sup>5</sup>	1.9×10 <sup>5</sup>
<b>3</b>	8.4×10 <sup>-4</sup> <sup>b</sup>	552; 589	553 <sup>f</sup> ; 585	7.6×10 <sup>4</sup>	9.8×10 <sup>4</sup>
<b>4b</b>	4.0×10 <sup>-4</sup> <sup>c</sup>	458	464	2.2×10 <sup>4</sup>	8.0×10 <sup>3</sup>
<b>5</b>	5.8×10 <sup>-3</sup>	349	350	3.2×10 <sup>4</sup>	5.0×10 <sup>4</sup>
<b>6</b>	1.9×10 <sup>-3</sup>	340	368	7.6×10 <sup>4</sup>	6.0×10 <sup>5</sup>
<b>7</b>	2.5×10 <sup>-2</sup>	317	331	3.5×10 <sup>4</sup>	8.4×10 <sup>2</sup>
<b>8</b>	1.2×10 <sup>-5</sup>	517	519	2.6×10 <sup>4</sup>	1.7×10 <sup>5</sup>
<b>9</b> {010}	9.1×10 <sup>-6</sup>	600	578	1.8×10 <sup>4</sup>	3.3×10 <sup>5</sup>
<b>9</b> {111}	9.1×10 <sup>-6</sup>	600	592	1.8×10 <sup>4</sup>	4.2×10 <sup>4</sup>
<b>10</b>	6.1×10 <sup>-5</sup>	503	506	2.7×10 <sup>4</sup>	1.4×10 <sup>5</sup>
<b>11</b> {110}	1.8×10 <sup>-4</sup> <sup>d</sup>	568 <sup>e</sup>	579	6.9×10 <sup>4</sup>	1.2×10 <sup>5</sup>
<b>11</b> {111}	1.8×10 <sup>-4</sup> <sup>d</sup>	568 <sup>e</sup>	565	6.9×10 <sup>4</sup>	2.5×10 <sup>5</sup>

<sup>a</sup> 9.1×10<sup>-3</sup>.<sup>b</sup> 1.0×10<sup>-2</sup> M H<sub>2</sub>SO<sub>4</sub>.<sup>c</sup> 1.0×10<sup>-1</sup>.<sup>d</sup> 7.8×10<sup>-2</sup> M KOH.<sup>e</sup> Basic solution.<sup>f</sup> Dimer absorption.<sup>g</sup> K<sub>2</sub>SO<sub>4</sub> solution.

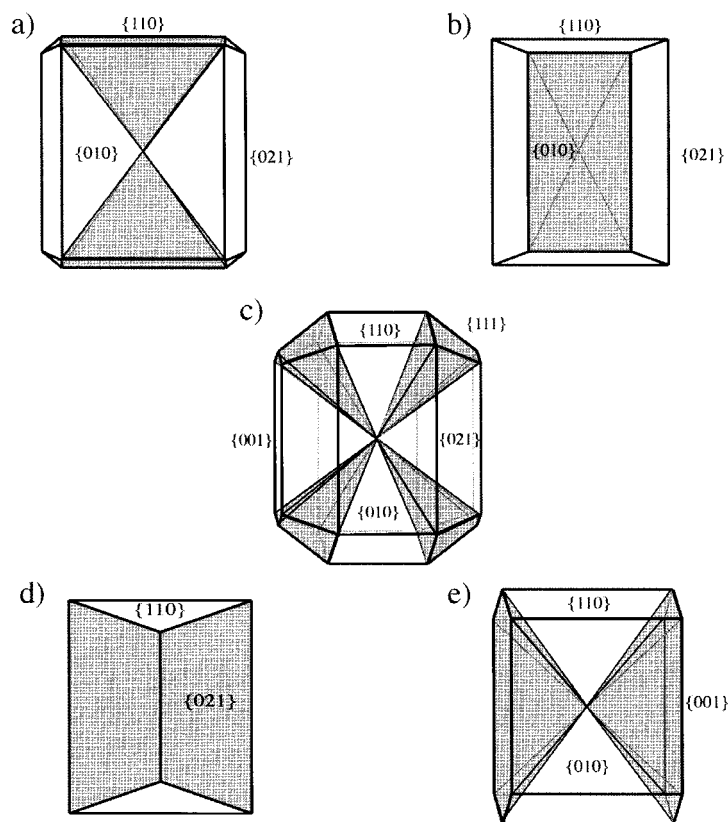


**Figure 1.** Representative habits of dyed  $K_2SO_4$  crystals. The shaded portions represent dyed sectors. (a) **1**, **2**, **3**, **8** or **11**; (b) **4**, **9** or **10**; (c) **9** or **11**; (d) **5**–**7**; (e) **7** or **12** in  $K_2SO_4$ .

showed, however, that at least some of Whetstone's models were incorrect because he did not have adequate knowledge of the geometries of the dye molecules.<sup>26</sup>

It was against this background that Addadi, Lahav, Leiserowitz and coworkers first succeeded in explaining the effects of additives on crystal form based on specific non-covalent interactions.<sup>27</sup> They emphasized amino acid and other hydrogen-bound molecular crystals; however, it

remains to be shown how the sulfonated dyes interact with growing sulfates. Despite the long-standing presumption of simplified electrostatic mechanisms for dye incorporation into salt crystals, experimental evidence is lacking. Previous structural judgements were based upon the indirect evidence of habit modification. Here, we test the  $-SO_3^- - SO_4^{2-}$  substitution mechanism by measuring the linear dichroism in a number of DICs, chemical systems in which the interactions of dye with crystal surfaces are not fleeting but fixed during

**Table 2.** C.I. numbers, dichroic ratios, experimental transition dipole moments from polarized absorption spectroscopy, and angles between calculated and experimental transition dipole moments of dyes in  $K_2SO_4$

Dye	C.I. number <sup>8</sup>	Dichroic ratios			Exp. transition moment <sup>a</sup>			Angle (°) <sup>c,d</sup>
		<i>alb</i>	<i>b/c</i>	<i>alc</i>	<i>x</i>	<i>y</i>	<i>z</i>	
<b>1<sub>r</sub></b>	42685	1.46	–	0.43	0.087	0.041	0.100	6
<b>1<sub>b</sub></b>	42685	1.97	–	0.84	0.106	0.043	0.089	18
<b>2</b>	45100	1.12	0.83	0.84	0.099	0.054	0.082	2
<b>3</b>	–	0.96	–	0.88	0.097	0.057	0.080	7
<b>4<sub>b</sub></b>	59040	–	0.00	0.00	0.130	0.000	0.000	1
<b>5</b>	–	0.29 <sup>b</sup>	4.40 <sup>b</sup>	0.28 <sup>b</sup>	0.038	0.087	0.056	9
<b>8</b>	16185	–	1.02	1.61	0.115	0.053	0.070	6 (33)
<b>9</b> / $\{111\}$	23850	–	0.75	0.86	0.099	0.053	0.083	18 (33)
<b>9</b> / $\{010\}$	23850	–	0.71	0.64	0.090	0.055	0.087	16 (37)
<b>10</b>	16575	0.59	–	0.49	0.080	0.059	0.088	16
<b>11</b> / $\{111\}$	23860	0.87	–	0.80	0.094	0.058	0.081	10 (29)
<b>11</b> / $\{110\}$	23860	0.99	0.81	0.87	0.099	0.055	0.082	8 (28)

<sup>a</sup> This is one transition moment in a family of four symmetry related experimental transition moments  $(x,y,z)$ ,  $(-x,y,z)$ ,  $(x,-y,z)$ ,  $(x,y,-z)$ .

<sup>b</sup> Values from polarized excitation spectroscopy.

<sup>c</sup> The numbers in parentheses are for models where all sulfonates were used in the least squares fit.

<sup>d</sup> The respective  $-SO_3^- - SO_4^{2-}$  distances in the refined models were as follows: **1**, 0.229, 0.373, 0.587 Å; **2**, 0.089, 0.089 Å; **3**, 0.145, 0.145 Å; **4**, 0.095, 0.203, 0.188 Å; **8**, 0.000, 0.000 Å; **9**, 0.105, 0.105 Å; **10**-model 1, 0.117, 0.117 Å; **10**-model 2, 0.149, 0.149 Å; **11**, 0.656, 0.535, 0.652, 0.538 Å.

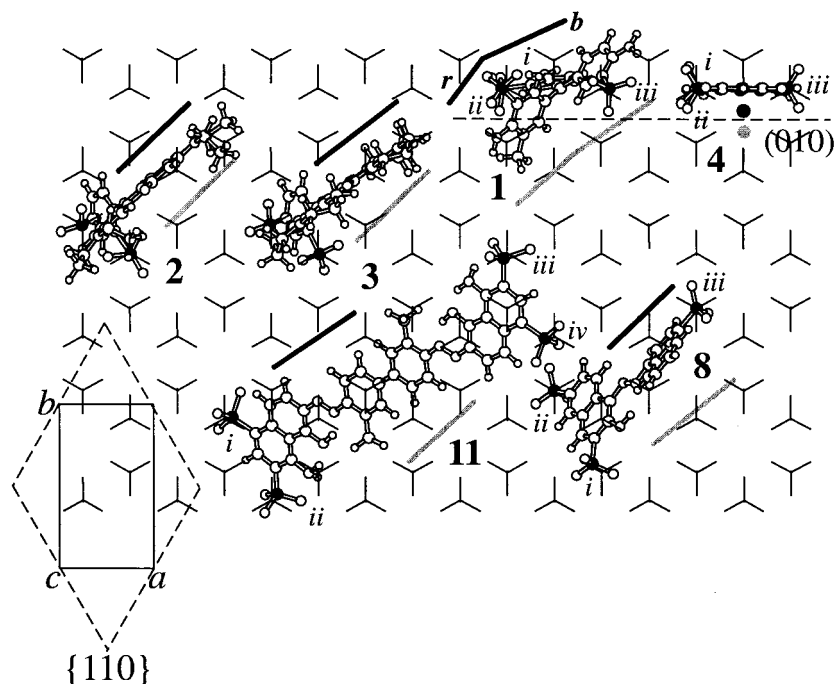


**Figure 2.** Representation of a  $K_2SO_4$  lattice containing **1**, **2**, **3**, **4**, **8** and **11**/**{110}** which recognize **{110}**.  $K^+$  ions deleted for clarity. The black and gray bars represent the calculated and experimental transition dipole moments, respectively. The dashed lines represent the **{110}** or **{010}** surface(s).

the process of mixed crystal formation. In conjunction with knowledge of the electronic transition dipole moments (ETDMs) of the molecules, we determined dye orientations. From this set of orientations we established translations of dye molecules with respect to the basis vectors of the host that are consistent with chemically sensible recognition mechanisms.

### General procedure

Dye inclusion crystals were grown by room temperature evaporation of aqueous  $K_2SO_4$  solutions containing dye (Table 1). Controlled crystallizations in constant temperature baths ( $30^\circ C$ ) were carried out to similar effect. The crystals displayed patterns of color corresponding to recognition of particular families of growth sectors (Fig. 1). The amount of dye incorporated in the crystals was quantified by measuring the absorbance of dissolved crystals (Table 1).

Crystals were cut, shaped, and polished with a string saw, sandpaper, and alumina grit, respectively. Linear dichroism was measured with a polarizing microscope based spectrophotometer (Table 2). The dye's ETDMs were calculated using the INDO/S-CI method<sup>28</sup> on MM2<sup>29</sup> or AM1<sup>30</sup> ground state conformations. The  $-SO_3^-$  sulfur atoms in the calculated dye structures were then least squares fit to the  $SO_4^{2-}$  sulfur atoms in the lattice. The angles between the experimental and theoretical ETDM best fits were calculated (Table 2). If the angles between the ETDMs were large ( $>30^\circ$ ), or had misfit distances ( $d_{S-S}$ ) between  $-SO_3^-$ – $SO_4^{2-}$  positions greater than  $0.5 \text{ \AA}$  the models were evaluated using fewer sulfonates (see models for **5**, **8**, **9** and **11**).

### Dye/ $K_2SO_4$ models

At room temperature  $K_2SO_4$  crystallizes in the orthorhombic space group  $Pnma$  with  $a=7.483 \text{ \AA}$ ,  $b=5.772 \text{ \AA}$ ,  $c=10.072 \text{ \AA}$ .<sup>4</sup> In order to be consistent with earlier researchers, we used the non-standard setting  $Pm\bar{c}n$  where  $b>c>a$ .<sup>31</sup> The vibration directions of orthorhombic crystals are parallel to the crystallographic axes. The birefringence ( $\Delta n=0.0038$ :  $n_x=1.4928$ ,  $n_y=1.4916$ , and  $n_z=1.4954$ ) is small obviating the need for refractive index corrections<sup>32</sup> to the polarized absorption spectra as these corrections resulted in a difference of less than 0.1%, well within the experimental error of the measurements.<sup>33</sup>

Of the approximately 100 dyes  $K_2SO_4$  incorporated, 11 were chosen for detailed investigation. Of these 11 dyes, we chose 2 tetrasulfonated dyes, 3 trisulfonated dyes, 4 disulfonated dyes, and 2 monosulfonated dyes. At least one dye for each of the principal growth sectors of  $K_2SO_4$  was studied. Of these 11 dyes, 9 recognized the **{110}** surface, 3 the **{010}**, 2 the **{111}**, 3 the **{021}**, and 1 the **{001}**.<sup>34</sup>

*Acid Fuchsin (1)* was the first dyed crystal that we reinvestigated.<sup>3,15,26,35</sup> It recognized the **{110}** growth sectors as first described by Buckley in 1934.<sup>11</sup> Mauri and Moret recently showed that **1** also recognized the **{010}** growth sectors of  $K_2SO_4$ .<sup>36</sup> Compound **1** has two equienergetic diastereomeric propeller conformations, one with approximately threefold symmetry and the other asymmetric. In the symmetric conformer, three sulfonates point to the same side of the mean molecular plane while the asymmetric conformer displays two sulfonates up and one down. The polarized absorption spectra coupled with conformational and spectroscopic analyses using semi-empirical molecular orbital calculations were consistent with the diastereospecific

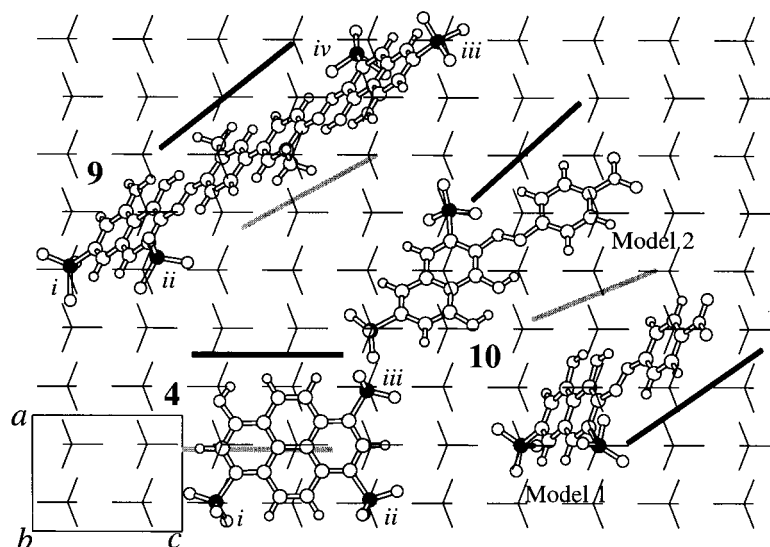


**Figure 3.** Representation of a  $\text{K}_2\text{SO}_4$  lattice containing **4**, **9**/ $\{010\}$  and **10** which recognize  $\{010\}$ .  $\text{K}^+$  ions deleted for clarity. The black and gray lines represent the calculated and experimental transition dipole moments, respectively.

incorporation of the asymmetric conformer where the sulfonate groups replaced sulfates in the lattice that are related to one another as the  $a$  and  $c$  lattice translations (Fig. 2).

*Sulforhodamine B* (**2**) was chosen as a guest for  $\text{K}_2\text{SO}_4$  because it has a large quantum efficiency for fluorescence; the mixed crystals were used as laser gain media.<sup>2a</sup> It also recognized the  $\{110\}$  growth sectors. The fluorescence spectra showed one peak with maximum intensity at 602 nm. However, the absorption spectra of the dyed crystal showed two peaks of equal intensity at 537 and 571 nm. These two absorptions were assigned to monomers and dimers, the fluorescence being quenched in the latter.<sup>37</sup>

The absolute orientation of **2**, a disulfonate, is not defined by  $-\text{SO}_3^- - \text{SO}_4^{2-}$  substitution. Rotation of the dye molecule about the  $-\text{SO}_3^- - \text{SO}_3^-$  vector in the lattice leaves the distances between S atoms unchanged. The molecule was rotated about this vector until we obtained a best match between experimental and theoretical moments (Fig. 2).

*Sulforhodamine 101* (**3**), a congener of **2**, also recognized the  $\{110\}$  growth sectors and had similar photophysical properties. Not surprisingly we obtained a comparable model for **3** and **2** (Table 2 and Fig. 2).

*Basic pyranine* (**4b**), a rigid analog of **1**, was also used as a laser gain medium in  $\text{K}_2\text{SO}_4$ .<sup>2a,3</sup> It recognized  $\{110\}$  as did **1** in addition to  $\{010\}$ . The orientations of the dye in the two growth sectors were indistinguishable with the ETDMs oriented parallel to the  $c$ -axis (Figs. 2 and 3). The phenoxide group was replaced with a variety of substituents varying in size and electronic properties, none of which precluded the incorporation in  $\text{K}_2\text{SO}_4$ ; all the dyes in this family were similarly oriented.

*2-Aminonaphthalene-1,5-disulfonate* (**5**) was recently the object of extensive investigations in our laboratories because of its long-lived room temperature phosphorescence.<sup>38</sup> The orientation was determined by measuring the

fluorescence intensity as a function of excitation polarization and by measuring the zero field splitting tensor of the triplet excited state by EPR spectroscopy. Together these results suggested an orientation that did not easily conform to a model in which  $-\text{SO}_3^- - \text{SO}_4^{2-}$  misfit distances were small. This judgement is fully supported by the fact that the *2-aminonaphthalenesulfonate* (**6**) and *2-aminobenzene-sulfonate* (**7**) also recognized  $\{021\}$  faces with a similar orientation. From this work we have surmised that not all sulfonate groups are used in determining dye orientations.<sup>39</sup>

*Amaranth* (**8**) in the  $\{110\}$  growth sectors was discovered by Buckley.<sup>12b</sup> Whetstone proposed a sulfonate-anion substitution model to explain the interaction of **8** with  $(\text{NH}_4)_2\text{SO}_4$ ,<sup>40</sup>  $\text{KNO}_3$ ,<sup>41</sup> and  $\text{NH}_4\text{NO}_3$ .<sup>24</sup> More recently, Lacmann and coworkers also explained the adsorption of **8** onto the  $\{010\}$  surface of  $\text{KNO}_3$  by invoking a Whetstone-like model.<sup>42</sup> We determined that the polarized absorption of **8** in  $\text{K}_2\text{SO}_4$  was not consistent with a model that minimized  $-\text{SO}_3^- - \text{SO}_4^{2-}$  distances of all three sulfonates (angle between experimental and calculated ETDMs was  $33^\circ$ ). However, the  $ii-iii - \text{SO}_3^- - \text{SO}_3^-$  distance (12.6 Å, see Fig. 2) matched a  $\text{SO}_4^{2-} - \text{SO}_4^{2-}$  distance in the  $\text{K}_2\text{SO}_4$  lattice. Superimposing rotating about the  $-\text{SO}_3^- - \text{SO}_3^-$  vectors in the standard way gave a minimum angle of  $6^\circ$ .

*Trypan blue* (**9**) recognized the  $\{111\}$  and  $\{010\}$  growth sectors (Fig. 1). Buckley noticed that similar large molecules such as brilliant congo R (**D**, C.I. # 23570), diamine sky blue A (**G**, C.I. # 24400), or diamine sky blue FF (**H**, C.I. # 24410) also preferred  $\{111\}$ .<sup>11</sup> The linear dichroism indicated that **9** was similarly oriented in both sectors, but these orientations were not consistent with a model that minimized  $-\text{SO}_3^- - \text{SO}_4^{2-}$  distances of three or four of the sulfonates (angular deviations between experimental and calculated ETDMs were  $33^\circ$  and  $37^\circ$  for  $\{111\}$  and  $\{010\}$  cases, respectively). Minimizing the  $-\text{SO}_3^- - \text{SO}_4^{2-}$  distances for sulfonates  $i$  and  $ii$  produced a model with  $18^\circ$  and  $16^\circ$  angular deviations for  $\{111\}$  and  $\{010\}$ , respectively (Figs. 3 and 4).

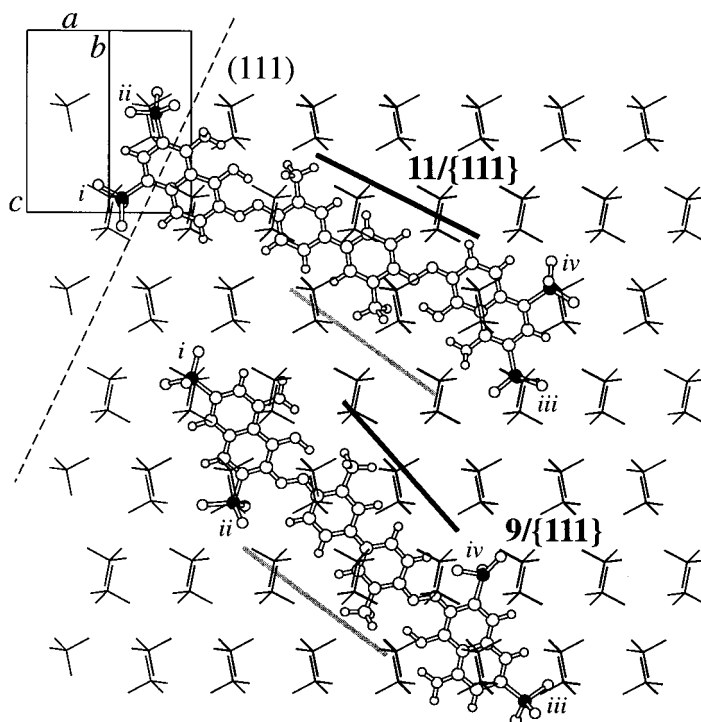


**Figure 4.** Representation of a  $K_2SO_4$  lattice containing  $9/\{111\}$  and  $11/\{111\}$  which recognize  $\{111\}$ .  $K^+$  ions deleted for clarity. The black and gray lines represent the calculated and experimental transition dipole moments, respectively. The dashed line represents the  $\{111\}$  surface. The symmetry related surfaces were omitted for clarity.

*Chromotrope 2B (10)* colored the  $\{010\}$  growth sectors.<sup>14</sup> Two comparable models were found: Model 1 has an angle of  $16^\circ$  between experimental and calculated ETDMs with a misfit distance of  $0.12 \text{ \AA}$  while model 2 has a slightly larger misfit distance ( $0.15 \text{ \AA}$ ) and an angular deviation between ETDMs of  $5^\circ$  (Fig. 3). In model 1, the orientation of the molecule is similar to that of **9**.

*Evan's blue (11)* colored the  $\{110\}$  growth sectors during early, rapid growth (Fig. 1a). Since the dihedral angle between the biaryl rings is highly variable, we allowed this parameter to take on that value which resulted in a best overlay of sulfonates and sulfates. This decision was supported by a Cambridge Structural Database (CSD)<sup>43</sup> search for biaryls without *ortho*-substituents. Of 381 hits, 149 had angles between  $0$  and  $15^\circ$ , 69 were between  $16$  and  $30^\circ$ , 146 structures were between  $31$  and  $45^\circ$ , and 17 were between  $46$  and  $60^\circ$ .<sup>44</sup>

Superposition of sulfates and sulfonates gave a reasonable agreement between the experimental and theoretical ETDMs ( $8^\circ$ ) as well as small average misfit lengths ( $0.60 \text{ \AA}$ ) (case 1, Fig. 2). However, there are three other sets of sulfates (cases 2–4) with comparable misfit lengths ( $0.41$ ,  $0.40$  and  $0.51 \text{ \AA}$  for cases 2, 3, and 4, respectively). Despite the geometrical similarities, these models were easily distinguished by the linear dichroism which gave angular mismatches between experimental and theoretical moments of  $8^\circ$  (case 1),  $36^\circ$  (case 2),  $28^\circ$  (case 3), and  $17^\circ$  (case 4) for  $11/K_2SO_4/\{110\}$ . During the later stages of crystallization, **11** colored  $\{111\}$  rather than  $\{110\}$  producing an X-shaped pattern resembling Buckley's 'Maltese Cross' for brilliant congo R in  $K_2SO_4$  (Fig. 1c).<sup>11</sup> The

polarized absorption spectra demonstrated that the dye was similarly oriented in the crystal despite different mechanisms at work during growth (Fig. 4); however, the absorption maxima of  $11/\{110\}$  were red-shifted by  $14 \text{ nm}$  relative to a basic aqueous solution of **11** and  $11/\{111\}$ .

### Habit modification

Buckley speculated that grouping the dyes in manageable, structurally coherent subsets would facilitate the discovery of the mechanisms of crystal habit modification. Toward this end he summarized the habit modifying powers of nine constitutionally isomeric dyes for six surfaces of five crystalline salts but apart from the tendency of the dyes to 'do something' their action was not easily correlated with constitution.<sup>12b</sup> Buckley, therefore, was not able to provide a molecular view of dyes interacting with crystal surfaces even though he realized that his observations undoubtedly contained structural information about the stereoselective interactions of organic dyes with growing crystal surfaces.

We compared the habits of the first  $K_2SO_4$  crystals grown by evaporation from aqueous solutions in Petri dishes containing  $5 \times 10^{-6} \text{ M}$  of dye and  $100 \text{ mL}$  aqueous saturated  $K_2SO_4$ . In the absence of dye the  $\{021\}$  faces were predominant. Small  $\{010\}$ ,  $\{110\}$ , and  $\{111\}$  faces were also evident. When any of the dyes that recognize the  $\{110\}$  sectors, **1**, **2**, **3**, **4**, **8** or **11**, were present in the growth solutions, the relative area of the  $\{110\}$  sectors increased. **3** and **11** also increased  $\{111\}$  while **4** and **11** increased  $\{010\}$ . The increase in the areas of  $\{110\}$  and  $\{111\}$  in the case of **11** was consistent with the fact that the dye recognized these two growth sectors. Similarly, **9** and **5**

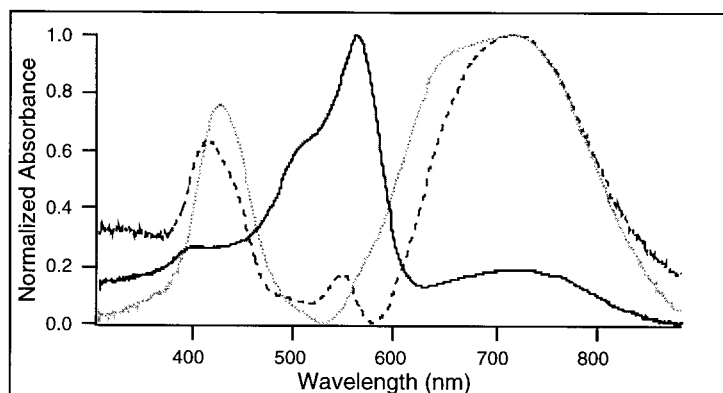


**Figure 5.** Visible absorption spectra of a mixed crystal of  $\text{K}_2\text{SO}_4$  containing **1** and **12**. The solid, dotted, and dashed lines represent spectra of the  $\{110\}$  sector,  $\{001\}$  sector, and growth solution, respectively.

increased the areas of  $\{111\}$  and  $\{021\}$ , respectively. These observations confirm the intuitive, dyed faces are slowed in their rate of growth.<sup>27</sup>

Buckley studied the habit modification of  $\text{K}_2\text{SO}_4$  in the presence of **1**, **8**, **9** and **11**. We obtained similar results as Buckley with **1** and **8**, but he needed higher concentrations (0.0030 g dye/1 g salt for **1** and 0.0003 g dye/1 g salt for **8**) to obtain the same effect. For **9**, Buckley saw an increase in  $\{010\}$ , but we saw an increase in  $\{111\}$ . Given that **9** recognized both faces, both observations are sensible. The factors that determine which face was modified are unknown at this time.

As concentrations of dyes in growth solutions were increased, habit changes were progressive. A particularly dramatic example is the effect of **4b** on  $\{010\}$ . Crystals from a  $5 \times 10^{-6}$  M **4b** solution have no  $\{010\}$  faces present. As the concentration of **4b** is increased ( $7 \times 10^{-6}$  M), the  $\{010\}$  appear and become dominant ( $8 \times 10^{-6}$  M) in thin tablets (compare habits in Fig. 1a, c, and d).

### Crystal growth as chromatography

There are several examples in the literature of bi-colored crystals grown in the presence of two or more dyes having different specificities for crystallographic surfaces.<sup>45</sup> We grew  $\text{K}_2\text{SO}_4$  crystals from muddy-brown aqueous solutions containing **1** ( $6.5 \times 10^{-5}$  M) and **12** ( $4.4 \times 10^{-4}$  M), that had alternately red  $\{110\}$  and green  $\{001\}$  growth sectors. Visible absorption spectra of individual sectors as compared with the growth solution showed that the  $\{110\}$  sectors contained only **1** while the  $\{001\}$  sectors contained only **12** (Fig. 5). Thus, the growing crystals separated a complex mixture. Similar results were obtained with **8** and **12**, and naturally can be extended to many of the dye pairs that recognize different faces.

### Isomorphous hosts

$\text{K}_2\text{SO}_4$  is one member of a family of isomorphous crystals including  $\text{K}_2\text{SeO}_4$ ,  $\text{K}_2\text{CrO}_4$ ,  $(\text{NH}_4)_2\text{SO}_4$ ,  $\text{Rb}_2\text{SO}_4$ , and  $\text{Cs}_2\text{SO}_4$ .<sup>4</sup> Crystals were grown from aqueous solutions of dyes **1–12** and the latter three salts whose unit cell volumes

increase with the cation size:  $435.0 \text{ \AA}^3$  ( $\text{K}_2\text{SO}_4$ );  $484.7 \text{ \AA}^3$  ( $\text{Rb}_2\text{SO}_4$ );  $495.8 \text{ \AA}^3$  ( $(\text{NH}_4)_2\text{SO}_4$ );  $527.9 \text{ \AA}^3$  ( $\text{Cs}_2\text{SO}_4$ ).  $\text{K}_2\text{SeO}_4$  ( $481.2 \text{ \AA}^3$ ) was excluded because it is highly toxic and costly; however, we did demonstrate that it could serve as host to **1**.<sup>33</sup>  $\text{K}_2\text{CrO}_4$  ( $468.5 \text{ \AA}^3$ ) was excluded because it is an oxidant. All the dyes colored crystals of  $\text{K}_2\text{SO}_4$  and  $\text{Rb}_2\text{SO}_4$  (except **11** which precipitated from  $\text{Rb}_2\text{SO}_4$  solutions).  $\text{Cs}_2\text{SO}_4$  was rarely colored and  $(\text{NH}_4)_2\text{SO}_4$  was never colored. The increase of volume from  $\text{K}_2\text{SO}_4$  to  $\text{Cs}_2\text{SO}_4$  is accompanied by an increase in the  $\text{SO}_4^{2-}$ – $\text{SO}_4^{2-}$  distances. Based upon our substitution mechanism, these increases in  $\text{SO}_4^{2-}$ – $\text{SO}_4^{2-}$  distances preclude the incorporation of dyes into  $\text{Cs}_2\text{SO}_4$  in some cases, but should encourage it in others. For example, **4b** substitutes for two  $\text{SO}_4^{2-}$  ions that are related by an *a* translation in the lattice. This distance becomes larger in the  $\text{Cs}_2\text{SO}_4$  lattice increasing the misfit distance between  $-\text{SO}_3^-$ – $\text{SO}_4^{2-}$  from  $0.172 \text{ \AA}$  in  $\text{K}_2\text{SO}_4$  to  $0.395 \text{ \AA}$  in  $\text{Cs}_2\text{SO}_4$ . In two cases, **2** and **3**, the  $-\text{SO}_3^-$ – $\text{SO}_4^{2-}$  distance *improves* as the lattice is expanded; however, the presumably requisite  $\{110\}$  faces are rarely present in  $\text{Cs}_2\text{SO}_4$ .<sup>31</sup> The dependence of incorporation of dyes upon the minimization of  $-\text{SO}_3^-$ – $\text{SO}_4^{2-}$  distances is supported by the fact that **7** which only needs one  $-\text{SO}_3^-$  group for incorporation colors  $\text{Cs}_2\text{SO}_4$ . Polarized absorption spectra of **4** and **9** in  $\{010\}$  of  $\text{Rb}_2\text{SO}_4$  indicated a similar orientation as in  $\text{K}_2\text{SO}_4$ . The inability of  $(\text{NH}_4)_2\text{SO}_4$  to adsorb and overgrow dyes is inexplicable at this time; however, we have observed that  $\text{KH}_2\text{PO}_4$  is far superior as a dye host to the isomorphous  $(\text{NH}_4)_2\text{HPO}_4$ .<sup>46</sup> This troublesome ‘ammonium effect’ is the subject of ongoing investigation.

### Discussion

The average value of the angle between experimental and theoretical ETDMs for dyes in  $\text{K}_2\text{SO}_4$  obtained by the model building procedure that emphasized, to the exclusion of all else, the minimization of  $-\text{SO}_3^-$ – $\text{SO}_4^{2-}$  distances, was  $18.3^\circ$ , and ranged from  $1$  to  $37^\circ$ . When the angle between experimental and calculated ETDMs was greater than  $30^\circ$  (the probability of one vector being randomly oriented within  $30^\circ$  of another vector or any of its three symmetry related partners in an *mmm* space group can be as high as 54%), the



models were reevaluated by exclusion of one or more of the sulfonates. This judgement was supported by the incorporation of congeners in similar orientations with fewer sulfonates. In this way the average value between experimental and theoretical ETDMs was reduced to  $9^\circ$ , and ranged from  $1$  to  $18^\circ$ . Given the probability that two randomly oriented vectors are aligned within some angle  $\theta$  is proportional to  $\int \sin \theta \delta \theta$ , the near parallelism does indeed suggest that there is considerable merit in the original suggestions of Buckley and France that  $-\text{SO}_3^-$ – $\text{SO}_4^{2-}$  substitution during crystal growth represents a dominant interfacial interaction. To place this judgement on a quantitative footing we calculated the probability in each case that a vector laid down in crystallographic space at random would fall within the smallest angular deviation ( $\theta$ ) of any of the symmetry related experimental ETDMs. This amounted to calculating the total area of four symmetry related disks ( $4(2\pi r^2(1-\cos \theta))$ ) within a hemisphere whose sizes were determined by  $\theta$  and then subtracting any overlapping area among the four which can be calculated as the sum of appropriate spherical triangles. The probability of a random vector falling within  $9^\circ$  of one of the symmetry related ETDMs was always less than 5%.

It must be pointed out that we have weighted the odds in our favor in several cases by choosing the biaryl angle in **9** and **11** as a parameter in the fitting procedures. At the same time, significant error is introduced generally through the use of gas phase dye structures for chromophores that may undergo conformational changes in the crystal, and by ignoring solvatochromism which must change the direction of the experimental transition moments of the chromophores. Moreover,  $-\text{SO}_3^-$  and  $\text{SO}_4^{2-}$  groups are not spheres of negative charge; the best electrostatic superpositions of  $-\text{SO}_3^-$  and  $\text{SO}_4^{2-}$  may not require vanishingly small  $-\text{SO}_3^-$ – $\text{SO}_4^{2-}$  distances. We did not account for the inevitable relaxation of the molecules first coordination sphere. Finally, hydrogen bonding and cation– $\pi$ <sup>47</sup> interactions are unavoidable in these mixed crystals.<sup>39</sup>

Nevertheless, Davey et al. have recently used contemporary molecular modeling software to support Whetstone's supposition that  $-\text{SO}_3^-$  groups substitute for  $\text{NO}_3^-$  ions by noting the close correspondence between these groups of atoms for some superpositions of one calculated dye structure onto the idealized  $\text{NH}_4\text{NO}_3$  lattice.<sup>48</sup> A similar interpretation was applied to the manner in which diphosphonates slow the growth of  $\text{BaSO}_4$  crystals.<sup>49</sup> Inhibition proceeded when the length of the flexible spacer joining the charged phosphonate groups enabled a two-point substitution for  $\text{SO}_4^{2-}$  ions on the crystal surface.

The aforementioned mechanism and the figures in this text presume idealized, flat, growing crystal surfaces. Better approximations would account for emergent secondary surface structures. We have seen by differential interference contrast microscopy that dyes can selectively recognize particular emergent structures on the faces of  $\text{K}_2\text{SO}_4$ ,  $\text{KH}_2\text{PO}_4$ , and  $\alpha$ -lactose monohydrate.<sup>39,50</sup> Mauri and Moret showed by in situ atomic force microscopy that **1** and **4** modify step morphologies on the  $\{110\}$  and  $\{010\}$  surfaces of  $\text{K}_2\text{SO}_4$ .<sup>36</sup> Bennema and coworkers<sup>51</sup> recently

used Hartman–Perdok theory to predict the habit and classify the faces of  $\text{K}_2\text{SO}_4$  as flat, stepped, or kinked. They failed to predict the morphological importance of the  $\{021\}$  faces, but this is reasonable given the gross topography of these faces that we have characterized elsewhere.<sup>39,50</sup>

Recently, Serra and coworkers adopted  $\text{K}_2\text{SO}_4$  as a host for several butanedione and pentanedione complexes of trivalent lanthanide ions such as  $\text{Eu}^{3+}$  and  $\text{Tb}^{3+}$ . They obtained hourglass patterns of luminescence associated with the  $\{110\}$  faces.<sup>52</sup> Obviously, in these cases the recognition mechanism is something other than sulfonate–sulfate substitution. Serra et al. postulated that  $\{110\}$  was recognized more often than any other face because it, unlike  $\{010\}$ ,  $\{021\}$ , and  $\{001\}$ , was composed of alternating layers of cations and anions. While electrostatic forces must be of paramount importance, we have identified groups of observations that support and refute a simple electrostatic interpretation. For example, the  $\{101\}$  surface of  $\text{KH}_2\text{PO}_4$  may be said to recognize anionic dyes in preference to  $\{100\}$  as it is a face terminated by  $\text{K}^+$  ions.<sup>37a,46,53</sup> Similarly, the cube faces of alum, having larger local fields, are dyed in preference to the octahedral faces.<sup>19a,b</sup> On the other hand, Frondel and Reinders dyed those faces of alkali halides that are composed of mixed cation and anion layers.<sup>54</sup>

## Conclusions

We have reinvestigated the orientation and overgrowth of sulfonated dyes by growing  $\text{K}_2\text{SO}_4$  crystals in order to assess the generality of a tacitly assumed recognition mechanism involving  $-\text{SO}_3^-$ – $\text{SO}_4^{2-}$  substitution. A simple model where the  $-\text{SO}_3^-$ – $\text{SO}_4^{2-}$  distances were minimized for all sulfonates was consistent with measured linear dichroism in 5 of 9 cases. However, we have shown that sometimes all sulfonates are not necessary for incorporation. Minimization of fewer  $-\text{SO}_3^-$ – $\text{SO}_4^{2-}$  distances in some cases can dramatically improve the model with respect to experiment. In one case the model does not seem to apply as the orientation of **11**/ $\text{K}_2\text{SO}_4$  could not be explained by the minimization of  $-\text{SO}_3^-$ – $\text{SO}_4^{2-}$  distances.

Can we make predictions? Yes. Can we expect to be successful more than 50% of the time? No. Of course, as there are many more ways of being wrong than right; we are in a better position than a coin tosser. Our ability to predict structure appears to be no better and no worse than that of traditional molecular crystal engineers relying on H-bond motifs.

## Experimental

### General methods

**1**, **6**, **7**, **9**, **11**, and **12** were purchased from Aldrich. **2** and **3** were purchased from either Aldrich or Kodak. **8** was purchased from Fischer Scientific. **4b** was formed by dissolving **4a** (Molecular Probes) in a KOH (Aldrich) solution. **5** was purchased from Matheson, Coleman & Bell. **10**

was purchased from Eastman Organic Chemicals. All dyes were used as received.

### Sample preparation and crystal indexing

In most cases, the spectra were obtained with light incident on well-developed faces and polarized in two orthogonal directions. In a few cases, the crystals were cut and shaped with South Bay Technology's Model 750 Acid Saw and 320 grit sandpaper followed by polishing with 0.3  $\mu\text{m}$  and/or 0.1  $\mu\text{m}$  alumina powder from Baikalo International Corporation. Crystals were indexed with a Stoe 2-circle Model J optical goniometer and a Nonius KappaCCD diffractometer.

### Molecular orbital calculations

The calculated transition dipole moments of each molecule were determined by applying an INDO/S-CI method<sup>28</sup> to the MM2<sup>29</sup> or AM1<sup>30</sup> optimized geometries.

### Absorption spectroscopy

Molar absorptivities were determined with a Hitachi U-2000 spectrophotometer controlled by Spectracalc software (Galactic Industries). Solution and crystal (isotropic and polarized) absorption spectra were obtained with SpectraCode's Multipoint Absorbance Imaging (MAI-20) Microscope. The instrument consists of an Olympus BX-50 polarizing microscope attached to an Acton Research Corporation Spectra Pro-300I triple grating monochromator by a fiber optic containing a linear array of 20 fibers. The monochromator is coupled to a Princeton Instruments' CCD detector. The spectrometer is controlled with KestrelSpec. The extinction directions of the biaxial crystals were used to orient the sample relative to the input polarization.

### Acknowledgements

The National Science Foundation (CHE-9457374, CHE-9727372) and the American Chemical Society Petroleum Research fund (30688-AC6) supported this work. We thank Jason Chow, Richard W. Gurney, Sei-Hum Jang, Mary Jennifer Jay, Scott Lovell, Michael P. Kelley, and Christine A. Mitchell for their published contributions acknowledged in the citations. Thanks also to John Toscano for access to the dissertations from the research group of Wesley France, The Ohio State University.

### References

- Nangia, A.; Desiraju, G. R. *Acta Crystallogr. Sect. A* **1998**, *54*, 934–944; Swift, J. A.; Reynolds, A. M.; Ward, M. D. *Chem. Mater.* **1998**, *10*, 4159–4168; Aakeröy, C. B. *Acta Crystallogr. Sect. B* **1997**, *53*, 569–586; MacDonald, J. C.; Whitesides, G. M. *Chem. Rev.* **1994**, *94*, 2383–2420.
- (a) Rifani, M.; Yin, Y.-Y.; Elliott, D. S.; Jay, M. J.; Jang, S.-H.; Kelley, M. P.; Bastin, L.; Kahr, B. *J. Am. Chem. Soc.* **1995**, *117*, 7572–7573. (b) Moerner, W. E.; Orrit, M. *Science* **1999**, *283*, 1670–1676. (c) Weiss, S. *Science* **1999**, *283*, 1676–1683.
- Kelley, M. P.; Janssens, B.; Kahr, B.; Vetter, W. M. *J. Am. Chem. Soc.* **1994**, *116*, 5519–5520.
- Wyckoff, R. W. G. *Crystal Structures*; Wiley Interscience: New York, 1965; Vol. 3, pp 95–97; Ojima, K.; Nishihata, Y.; Sawada, A. *Acta Crystallogr. Sect. B* **1995**, *51*, 287–293.
- Sénarmont, H. *Ann. Phys. (Leipzig)* **1854**, *167*, 491–494.
- Kny, L. *Ber. Dtsch. Bot. Ges.* **1887**, *5*, 387–395.
- Retgers, J. W. *Zeit. Physikal. Chem.* **1893**, *12*, 583–622.
- The *Colour Index*, a catalog of commercial dyes containing structures and numerical dye identifiers (C.I. #s), was not compiled until 1924 (Rowe, F. M., Ed. *Colour Index*, Society of Dyers and Colourists, Bradford, 1924), therefore we cannot know whether old dyes correspond to compounds of the same name that are commercially available today. The current 3rd edition (1971) of the *Colour Index* uses a different indexing system. A conversion between the conventions in the 1st and 3rd editions can be found in the 2nd edition (1956).
- Wenk, W. *Zeit. Krist.* **1910**, *47*, 124–162.
- Gaubert, P. *Comptes. Rendus.* **1912**, *155*, 649–651; see also: Neuhaus, A. *Angew. Chem.* **1941**, *54*, 527–536.
- Buckley, H. E. *Zeit. Krist.* **1934**, *88*, 122–127 (see also p 248–255).
- (a) Buckley, H. E.; Cocker, W. *Zeit. Krist.* **1933**, *85*, 58–73. (b) Buckley, H. E. *Zeit. Krist.* **1934**, *88*, 381–411. (c) **1935**, *91*, 375–401; (d) *Dis. Faraday Soc.* **1949**, *5*, 243–254.
- The general idea of using dyes to influence the habit of crystals was borrowed from Gaubert. See, for example: Gaubert, P. *Rev. Gen. Sci.* **1926**, *37*, 357–366.
- Buckley, H. E. *Mem. Proc. Manchester Lit. Philos. Soc.* **1951**, *92*, 77–123.
- For a critical evaluation of Buckley's habit modification studies, see: Kelley, M. P.; Chow, J. K.; Kahr, B. *Mol. Cryst. Liq. Cryst.* **1994**, *242*, 201–214.
- Freund, I. *The Study of Chemical Composition. An Account of Its Method and Historical Development*, Dover: New York, 1968; Chapter 15.
- Buckley, H. E. *Mem. Proc. Manchester Lit. Philos. Soc.* **1938–1939**, *83*, 31–62.
- Buckley, H. E. *Crystal Growth*, Wiley: New York, 1951; pp 422.
- (a) Keenan, F. G.; France, W. G. *J. Am. Ceram. Soc.* **1927**, *10*, 821–827. (b) Bennett, G. W.; France, W. G. *J. Am. Ceram. Soc.* **1928**, *11*, 571–581. (c) Lash, M. E.; France, W. G. *J. Phys. Chem.* **1930**, *34*, 724–736; see also: France, W. G. *Colloid Symp. Ann.* **1930**, *7*, 59–87; Weinland, L. A.; France, W. G. *J. Phys. Chem.* **1932**, *36*, 2832–2839; Paine, P. A.; France, W. G. *J. Phys. Chem.* **1935**, *39*, 425–429; Davis, P. P.; France, W. G. *J. Phys. Chem.* **1936**, *40*, 81–87; France, W. G.; Wolfe, K. M. *J. Phys. Chem.* **1941**, *45*, 395–401; France, W. G.; Wolfe, K. M. *J. Am. Chem. Soc.* **1941**, *63*, 1505–1507. The theses of France's students are also a valuable resource: Eckert, T. S. Ph.D Dissertation, The Ohio State University, 1925; Keenan, F. G. Ph.D, 1926; Lash, M. E. Ph.D, 1928; Foote, F. G. M.S., 1929; Weinland, L. A., Ph.D 1930; Paine, P. A. M.S., 1933; Paine, P. A. Ph.D, 1934; Rigtterink, M. D. Ph.D, 1937; Wolfe, K. M. Ph.D, 1938.
- Rigtterink, M. D.; France, W. G. *J. Phys. Chem.* **1938**, *42*, 1079–1088.
- Foote, F. G.; Blake, F. C.; France, W. G. *J. Phys. Chem.* **1930**, *34*, 2236–2240.
- Vetter, W.; Dudley, M.; Kahr, B. In *National Synchrotron Light Source Report*; Hurlburt, S. L., Lazarz, M. L., Eds.; Brookhaven National Laboratory: Upton, New York, 1993; p B169; Kelley, M. P.; Kahr, B.; Dudley, M. In *National*

*Synchrotron Light Source Report*, Rothman, E. Z., Ed.; Brookhaven National Laboratory: Upton, New York, 1994; p B132.

23. Whetstone, J. *Ind. Eng. Chem.* **1952**, *44*, 2663–2667; *British Patent* 665,478, **1953**.
24. Whetstone, J. *Disc. Faraday Soc.* **1954**, 132–140.
25. Whetstone, J. *J. Chem. Soc.* **1956**, 4841–4847.
26. Kahr, B.; Kelley, M. P. In *Supramolecular Stereochemistry*; Siegel, J. S., Ed.; Kluwer: Netherlands, 1995, pp 203–221.
27. Addadi, L.; Berkovitch-Yellin, Z.; Weissbuch, I.; Lahav, M.; Leiserowitz, L. *J. Am. Chem. Soc.* **1982**, *104*, 2075–2077; Addadi, L.; Berkovitch-Yellin, Z.; Weissbuch, I.; Mil, J. v.; Shimon, L. J. W.; Lahav, M.; Leiserowitz, L. *Angew. Chem. Int. Ed. Engl.* **1985**, *24*, 466–485; Addadi, L.; Berkovitch-Yellin, Z.; Weissbuch, I.; Lahav, M.; Leiserowitz, L. In: *Topics in Stereochemistry*; Eliel, E. L., Willen, S. H., Allinger, N. L., Eds.; Wiley: New York, 1991; pp 1–85; Vaida, M.; Shimon, L. J. W.; Weisinger-Lewin, Y.; Frolow, F.; Lahav, M.; Leiserowitz, L.; McMullan, R. K. *Science* **1988**, *241*, 1475–1479; Weissbuch, I.; Popovitz-Biro, R.; Lahav, M.; Leiserowitz, L. *Acta Crystallogr. B* **1995**, *51*, 115–148.
28. Ridley, J.; Zerner, M. *Theor. Chim. Acta* **1973**, *32*, 111–134; Ridley, J. E.; Zerner, M. C. *Theor. Chim. Acta* **1976**, *42*, 223–236.
29. Allinger, N. L. *Am. Chem. Soc.* **1977**, *99*, 8127–8134.
30. Dewar, M. J. S.; Zebisch, E. G.; Healy, E. F.; Stewart, J. J. P. *J. Am. Chem. Soc.* **1985**, *107*, 3902–3909; Stewart, J. J. P. *Quantum Chemistry Program Exchange*, Bloomington, IN, No. 455.
31. Groth, P. *Chemische Krystallographie*; Wilhelm Engelmann: Leipzig, 1908; Vol. 2, pp 337–340; Tutton, A. E. *J. Chem. Soc.* **1894**, 628–717.
32. Winchell, A. N.; Winchell, H. *The Microscopical Characters of Artificial Inorganic Solid Substances: Optical Properties of Artificial Minerals*; McCrone Research Institute; Chicago, 1989, p 125.
33. Kelley, M. M.Sc. Thesis, Purdue University, 1997, p 15.
34. Tutton, Groth, and Buckley reported small, rare facets including: {011}, {031}, {130}, {112}, and {100}. We observed them infrequently. See Ref. 31 and Buckley, H. E. *Zeit. Krist.* **1932**, *81*, 157–168.
35. Kahr, B.; Chow, J. K.; Peterson, M. L. *J. Chem. Ed.* **1994**, *71*, 584–586.
36. Mauri, A.; Moret, M. *J. Cryst. Growth* **2000**, *208*, 599–614.
37. (a) Kahr, B.; Jang, S.-H.; Subramony, J. A.; Kelley, M. P.; Bastin, L. *Adv. Mat.* **1996**, *8*, 941–944. (b) Chambers, R. W.; Kajiwar, T.; Kearns, D. R. *J. Phys. Chem.* **1974**, *78*, 380–387.
38. Mitchell, C. A.; Gurney, R. W.; Jang, S.-H.; Kahr, B. *J. Am. Chem. Soc.* **1998**, *120*, 9726–9727.
39. Gurney, R. W.; Mitchell, C. A.; Ham, S.; Bastin, L. D.; Kahr, B. *J. Chem. Phys. B* **2000**, *104*, 878–892.
40. Whetstone, J. *J. Chem. Soc.* **1957**, 4289–4294.
41. Whetstone, J. *J. Chem. Soc.* **1957**, 4284–4289.
42. Kipp, S.; Lacmann, R.; Rolfs, J. *J. Cryst. Growth* **1997**, *171*, 183–189; Rolfs, J. Dissertation, University of Braunschweig, 1992.
43. *Cambridge Structural Database*, version 2.3.7; see: Allen, F. H.; Kennard, O.; Taylor, R. *Acc. Chem. Res.* **1983**, *16*, 146–153; Allen, F. H.; Bellard, S.; Brice, M. D.; Cartwright, B. A.; Doubleday, A.; Higgs, H.; Hummelink, T.; Hummelink-Peters, B. G.; Kennard, O.; Motherwell, W. D. S.; Rogers, J. R.; Watson, D. G. *Acta Crystallogr. B* **1979**, *35*, 2331–2339.
44. For a previous CSD study of biaryl geometries see: Brock, C. P.; Minton, R. P. *J. Am. Chem. Soc.* **1989**, *111*, 4586–4593.
45. Gaubert, P. *Ann. Rep. Smithsonian Inst. 1909* **1910**, *29*, 271–278. *Bull. Soc. Fr. Min.* **1902**, *25*, 223–260. *Comptes Rendus* **1907**, *145*, 378–380; see also: Paine, P. A. 1993, Ref. 19.
46. Subramony, J. A. Ph.D Dissertation, Purdue University, 1999.
47. Ma, J. C.; Dougherty, D. A. *Chem. Rev.* **1997**, *97*, 1303–1324.
48. Davey, R. J.; Polyskwa, L. A.; Maginn, S. J. In *Adv. Ind. Cryst.*, Garside, J., Davey, R. J., Jones, A. G. Eds.; Butterworth-Heinemann: Oxford, 1991, pp 150–165.
49. Davey, R. J.; Black, S. N.; Bromley, L. A.; Cottier, D.; Dobbs, B.; Rout, J. E. *Nature* **1991**, *353*, 549–550; Rohl, A. L.; Gay, D. H.; Davey, R. J.; Catlow, C. R. A. *J. Am. Chem. Soc.* **1996**, *118*, 642–648; Coveney, P. V.; Davey, R. J.; Griffin, J. L. W.; Whiting, A. *J. Chem. Soc., Chem. Commun.* **1998**, 1467–1468.
50. Gurney, R. W.; Kurimoto, M.; Subramony, J. A.; Bastin, L. D.; Kahr, B. *ACS Symp. Ser.* **2000** (Glaser, R.; Kaszynski, P. eds.).
51. Vogels, L. J. P.; Verheijen, M. A.; Bennema, P. *J. Cryst. Growth* **1991**, *110*, 604–616.
52. Serra, O. A.; Rosa, I. L. V.; Nassar, E. J.; Calefi, P. S.; Cardoso, P. C. *J. Alloys and Compounds* **1997**, *249*, 178–180; Serra, O. A.; Rosa, I. L. V.; Nassar, E. J.; Cardoso, P. C. *J. Rare Earths (Special Issue)* **1995**, 206; Serra, O. A.; Nassar, E. J.; Kodaira, C. A.; Calefi, P. S.; Rosa, I. L. V. *Spectrochim. Acta, Part A* **1998**, *54*, 2077–2080.
53. de Vries, S. A.; Goedtkindt, P.; Bennett, S. L.; Huisman, W. J.; Zwanenburg, M. J.; Smilgies, D.-M.; De Yoreo, J. J.; van Enkevort, W. J. P.; Bennema, P.; Vlieg, E. *Phys. Rev. Lett.* **1998**, *80*, 2229–2232.
54. Frondel, C. *Am. Min.* **1940**, *25*, 91–110; Reinders, W. *Zeit. Physikal. Chem.* **1911**, *77*, 213–226, 677–699; Reinders, W. *Z. Chem. Ind. Kolloide* **1912**, *9*, 10–14.